RSC Advances

PAPER

View Article Online
View Journal | View Issue

Cite this: *RSC Adv.*, 2021, **11**, 2377

CH/π-interaction-driven self-assembly of tetraphenylethylene derivatives into the face to face arrangement†

Lirong Yu,‡[a] Mengxing Zhang,‡[a] Dandan Lou,[a] Jiale Li,[a] Xi Wang *[a] and Ming Bai *[ab]

For tetraphenylethene (TPE) derivatives, it is difficult to determine the arrangement of the molecules in the aggregation state because disordered aggregation usually occurs. To solve the problem, we have explored a novel and facile strategy to investigate the aggregation mode of a TPE derivative framework in which the two neighboring *ortho* carbons of two phenyl moieties at the same ethylene carbon were linked with an alkoxyl chain (C4) (denoted as **TPEC4**). The XRD measurements on the particles obtained in a DMSO/H_2O mixture (f_w = 60%) showed sharp peaks which is consistent with the simulated XRD patterns on the basis of a single crystal structure of **TPEC4**, indicating well-ordered molecular packing in the aggregated state. The CH/π-interaction and solvophobicity driven self-assembly behaviour of the compound was observed in the DMSO/H_2O mixture. A face to face molecular packing structure that arises from quadruple intermolecular CH/π-interactions of the tetraphenylethylenes is the key motif for self-assembly in solution. The unique blue-red shifted emission in the DMSO/H_2O mixture associated with aggregated behaviour of the compound was also investigated. This discovery will provide the basis for theoretical research and the rational design of TPE-based luminogens.

Received 16th December 2020
Accepted 28th December 2020

DOI: 10.1039/d0ra10572d

rsc.li/rsc-advances

Introduction

Tetraphenylethene (TPE) derivatives have been attracting increasing research interest in the past decade because of their intriguing aggregation-induced emission (AIE) properties.[1–6] The intramolecular rotation, vibration and photoisomerization *via* a π bond twist of TPE luminogens have been efficiently suppressed in the solid state, which then blocks the radiationless relaxation channel, opens the radiative decay pathway,[7,8] and allows TPE to emit efficiently in a concentrated state, endowing TPE derivatives with diverse application potentials in organic light-emitting, biosensing, fluorescent sensors, and biological probes.[9]

As aggregation induced emission luminogens, the driving forces or the methodologies of aggregation are very important not only because they can open the radiative decay pathway but also because the packing status in the aggregate state could affect the emission properties of AIE luminogens.[10,11] To aggregation process, the AIE luminogens, especially TPEs, were typically driven self-organized singly or multiply by weak non-covalent interactions, such as solvophobic effects, host–guest interaction, metal–ligand coordination, intermolecular π–π interactions, electrostatic interactions, and hydrogen bonding interactions *etc.*[12,13]

CH/π interactions, a type of weak hydrogen bond, in which the energy associated with CH/π interactions are much smaller (0.8 kcal mol^{-1}) relative to that of typical strong hydrogen bonding interactions between H–O···H or H–N···H (3.5 to 7.8 kcal mol^{-1}) and the average distance between the C-donor and π-acceptor was observed to be longer than 2.5 Å.[14] But these weak bonds contribute significantly to the conformation and stability of 3D structures of biological macromolecules as well as in many molecular recognition events.[15,16] Interestingly, it was also found to be strong enough to drive molecules in a particular conformation to produce higher-order self-assembly.[14,17–19] Although massive intermolecular CH/π interactions exist which can help to restrict the free rotational motions of the phenyl rings of TPE,[10,11] the CH/π-interaction-induced molecular self-assembly in the TPE systems has not been reported.

In our previous work, the alkoxyl chains with different length ranging from one to four carbons are employed to link the two phenyl moieties on one end of ethylene in the TPE frameworks, resulting in a successful regulation over the molecular conformation.[20] Among the series compounds, the compound **TPEC4**

[a]*Marine College, Shandong University, Weihai, Weihai 264209, People's Republic of China. E-mail: xi_wang@sdu.edu.cn; ming_bai@sdu.edu.cn*

[b]*SDU-ANU Joint Science College, Shandong University, Weihai, Weihai 264209, People's Republic of China*

† Electronic supplementary information (ESI) available: Experimental details and spectroscopic data. CCDC 2019817. For ESI and crystallographic data in CIF or other electronic format see DOI: 10.1039/d0ra10572d

‡ These authors contributed equally to this work.

showed a unique blue-red shifted emission property in mixtures of H_2O/DMSO with different water fractions (f_w, the volume percentage of H_2O in the H_2O/DMSO mixture). In this work, combing the powder XRD patterns of the particles formed in DMSO/H_2O mixture with f_w = 60% and the single crystals structure of **TPEC4** which was obtained in mixed THF and methanol (3/1, v/v), we found that in the aggregation state with shorter wavelength emission, the two **TPEC4** enantiomers adopt a face to face arrangement with a lightly offset in crystal state. Encouragingly, the quadruple CH/π interactions exist between the adjacent TPE molecules which dominate the self-assembly of the **TPEC4** molecules together with solvophobic effect. The relation between the luminescent property and the structure was further investigated.

Experimental

Reagents

Tetrahydrofuran (THF) was distilled from sodium wire and benzophenone under nitrogen. Dichloromethane (DCM) was distilled from CaH_2. Column chromatography was carried out on a silica gel column (Qingdao Haiyang, 200–300 mesh) with the indicated eluents. All the other reagents such as benzophenone, *n*-butyllithium in hexane (2.5 mol L^{-1}), 2,2′-dihydroxybenzophenone, diphenylmethane, methyl iodine, diiodomethane, 1,2-dibromoethane, 1,3-dibromopropane, 1,4-dibromobutane were used as received.

Instrumentation

^{1}H NMR spectra were recorded on a Bruker DPX 400 spectrometer (^{1}H: 400 MHz, ^{13}C: 100 MHz) in $CDCl_3$. Spectra were referenced internally using the residual solvent resonances (δ = 7.28 for ^{1}H NMR) relative to $SiMe_4$ (δ = 0 ppm). ^{13}C NMR spectra were referenced internally by using the solvent resonances (δ = 77.00 ppm for $CDCl_3$). Electronic absorption spectra were recorded on a Hitachi U-2900 spectrophotometer. Steady-state fluorescence spectra were recorded on a Hitachi F-7000 spectrophotometer and an Edinburgh Instruments FLS920 three-monochromator spectrophotometer. The emission spectra were corrected for the wavelength dependence of the sensitivity of the detection system. The absolute fluorescence quantum yields were measured with an integrating sphere. Fluorescence images were taken on a Nikon Eclipse Ti florescence microscope. ESI-MS spectrum was taken on a Thermo Fisher Q-Exactive mass spectrometer. Single-crystal X-ray diffraction analyses were performed on an Aglient Super Nova Atlas Dual diffractometer using CuKα radiation (λ = 1.54184 Å). Structure was solved by direct methods using SHELXTL and refined by full-matrix least-squares on F^2 using SHELX-97. Non-hydrogen atoms were refined with anisotropic displacement parameters during the final cycles. Hydrogen atoms were placed in calculated positions with isotropic displacement parameters set to 1.2 × U_{eq} of the attached atom. Crystallographic data (excluding structure factors) for the structures reported in this paper have been deposited in the Cambridge Crystallographic Data Center with CCDC Number: 2019817.

^{1}H NMR and ESI-MS

Compound **TPEC4**. Yield: 92% (white powder). ^{1}H NMR (400 MHz, $CDCl_3$), δ (TMS, ppm): 7.08–7.04 (m, 14H, ArH), 6.79 (t, 2H, J = 7.2 Hz, ArH), 6.75 (d, 2H, J = 8.0 Hz, ArH), 4.33 (s, 2H, –OCH_2–), 4.11 (s, 2H, –OCH_2–), 1.97 (s, 2H, –CH_2–), 1.97 (s, 2H, –CH_2–). ^{13}C NMR (100 MHz, $CDCl_3$), δ: 156.03, 142.97, 142.17, 134.52, 134.03, 131.09, 130.48, 127.58, 127.10, 126.04, 120.71, 115.31, 69.96, 26.97. ESI-MS: found an isotopic cluster peaking at m/z [M + H^+] 419.17; calculated for $C_{30}H_{26}O_2$, 419.20.

Results and discussion

Luminescent properties of TPEC4 in DMSO/H_2O mixture

As shown in previous work, to investigate the AIE activity and the emission properties of **TPEC4**, the fluorescence and electronic absorption spectra in DMSO/H_2O with different water fractions were studied.[20] As shown in Fig. 1, a weak emission at 425 nm could be found in the enlarged spectrum of **TPEC4** in DMSO due to the restriction in part for the alkoxyl chain. When the f_w increases from 0 to 30%, the emission showed a slightly red shifted emission from 425 to 433 nm without obvious changes in intensity. With the f_w increasing from 30% to 60%, the fluorescence emission gets increased in a swift manner. A blue-shifted emission from 433 to 395 nm was observed. But the value of f_w from 0 to 55%, the absorption band of the solution

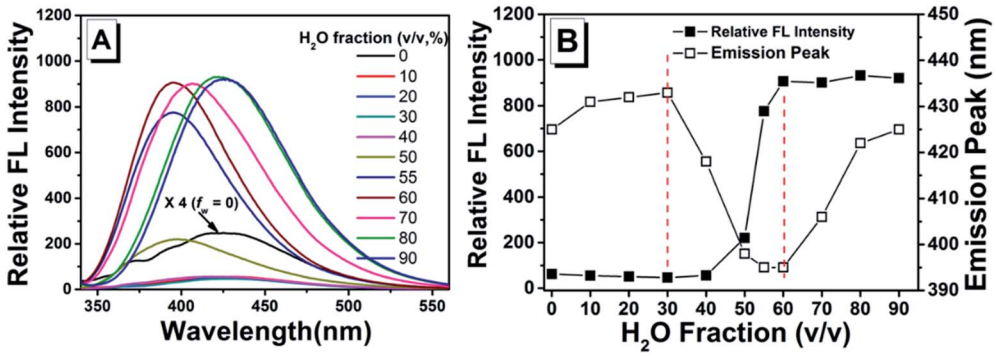

Fig. 1 (A) Fluorescence spectra and (B) plots of the emission peak and fluorescence intensity at maximum emission of **TPEC4** in DMSO/H_2O mixtures with different water fractions. Concentration: 50 μM; λ_{ex}: 330 nm (5 nm, 5 nm); 293 K.

does not change obviously with $\lambda_{max} \approx 286$ nm (Fig. S1, ESI†) which is not consisted with the phenomena of typical H-aggregation. After the f_w gets over 70%, the **TPEC4** exhibits a red-shift emission from 395 to 425 nm again with the absorption λ_{max} changed from 286 to 292 nm. The wavelength of emission peak in $f_w = 90\%$ is identical to $f_w = 0$. The fluorescence spectra of **TPEC4** in DMSO in different concentration (0.5 to 800 μM) were also recorded (Fig. S2, ESI†). With the concentration increasing, the emission peak located at about 425 nm with increasing intensity. By plotting the fluorescence intensity *versus* the concentration, a nonlinear line is obtained (Fig. S2B, ESI†), indicating that compound **TPEC4** is aggregated under these conditions.

Structure and luminescent properties of TPEC4-THF compared with TPEC4-DCM in crystal state

Fortunately, the single crystals of **TPEC4** were obtained in mixed THF and methanol (3/1, v/v) *via* slow evaporation (denoted as **TPEC4-THF**). The packing model of the **TPEC4** molecules in crystal is different from our previous report, in which the reported crystal is obtained in CH_2Cl_2 and methanol mixed solvent (**TPEC4-DCM**; CCDC number: 1820144; Fig. S7, ESI†).[20] The detailed crystallographic data of the two kinds of crystals which crystallized in different space groups are listed in Table S1 (ESI†). As shown in Fig. 2A and B, compound **TPEC4-THF** exists as a pair of conformational enantiomers in a unit cell. Table S2 (ESI†) compares the dihedral angles formed between the four phenyl moieties and the C=C bond of **TPEC4** in *P* conformation (Fig. S5†) (the nomination of the conformational enantiomers is presented in Fig. S4, ESI†). The dihedral angles between the four phenyl rings and the C=C bond in **TPEC4**, ranging from 38.071(106) to 68.978(72)° (Table S2, ESI†). No obvious luminescence of the single solid crystals was observed under bright field, however, the single crystals become to emit strong blue light under UV irradiation (wavelength: 330–380 nm) (Fig. 2C and D).

To point out the driven force for such arrangement of TPE moiety in **TPEC4-THF**, the intramolecular/intermolecular interaction was further investigated. The intramolecular hydrogen bonding interactions of C–H···O (2.725 Å) existed in each molecule, however, no typical intermolecular hydrogen bonds were observed (Fig. S6, ESI†). Therefore, the other weak non-covalent interactions could possibly induce the assembly of the compound with such twist molecular conformation. It can be seen from Fig. 3A, there are two different types of CH/π interactions existed in this compound, including the interactions within one unit cell and between adjacent unit cells. In one unit cell, CH/π interactions occur in a nearly vertical direction between the hydrogen atoms (2-position) of one benzene ring linked to the alkoxyl chain (donor) and the benzene plane arranged at the diagonal position of the former benzene ring in the adjacent molecule (acceptor). The resulted nonbonding H···C distances is about 2.709 Å and such interaction is donated as Type I CH/π interaction. Between the adjacent unit cells, the C–H bond located at 2-position of the benzene ring which act as an acceptor in the above Type I interaction is nearly perpendicular to the neighbouring benzene plane. Between the neighbouring molecules, the

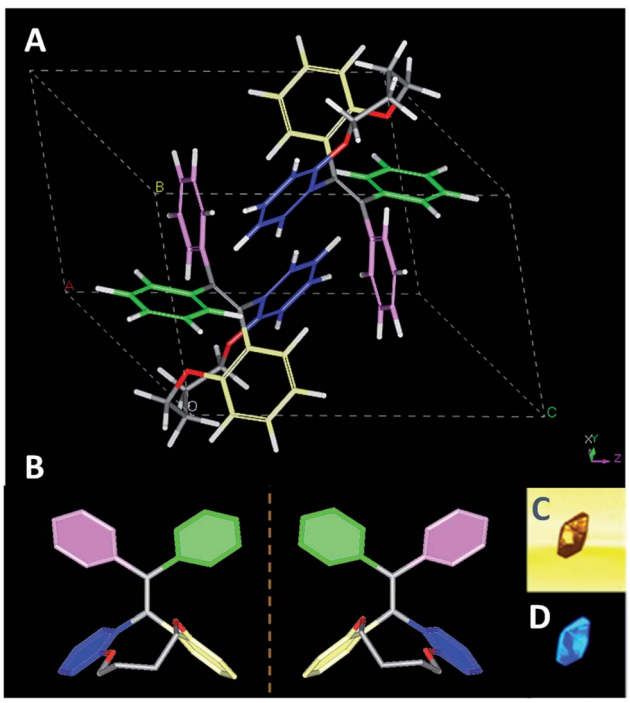

Fig. 2 (A) The structure of TPEC4-THF molecular in a unit cell and (B) a pair of conformational enantiomer existed in a unit cell with non-related hydrogens omitted for clarity; the images of crystals under bright field (C) and UV-light irradiation (D) (wavelength: 330–380 nm).

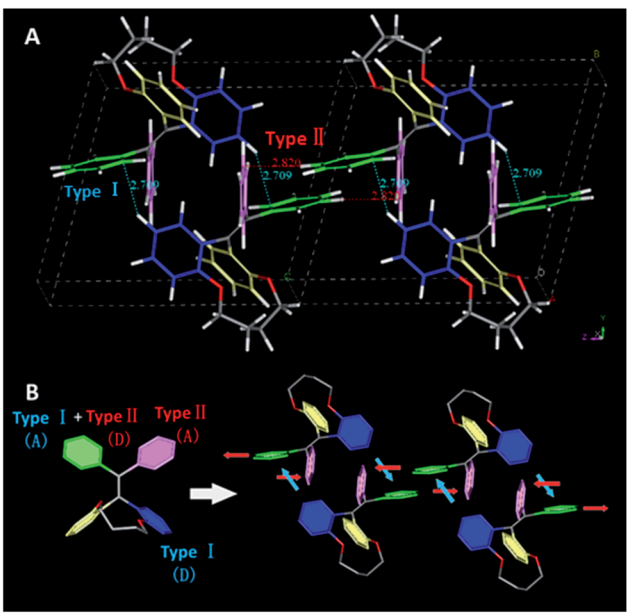

Fig. 3 The intermolecular CH/π-interactions in TPEC4-THF (A), including the interaction within one unit cell (Type I) and the interaction between the adjacent unit cells (Type II); schematic representation of the CH/π-interactions that leads to the self-assembly of TPEC4-THF (B).

shortest nonbonded distance between H provided by C–H bond (2-position) and C existed in the vertical plane is 2.820 Å. This C–H-donor/π-acceptor system is the second kind of CH/π-interactions, which donated as Type II interaction. Fig. 3B shows schematic representation of the CH/π-interactions clearly, in which the staggered quadruple intermolecular CH/π-interactions formed. That is, the two kinds of different perpendicular t-shaped CH/π bonds between the adjacent molecules distributed throughout the whole structure. To the best of our knowledge, generally, TPE molecules were regarded as adopting highly twisted molecular conformations which reduced or eliminated the face to face π–π stacking between the adjacent TPE molecules.[21] In this structure, similarly, the dominated CH/π interaction make the two molecules of **TPEC4-THF** adopted a face to face arrangement with a lightly offset. It is worth mentioning further that besides the weak non-covalent interactions play an important role in the self-assembly, the solvophobic effect should also be considered. The distinctly different packing model of the **TPEC4-THF** and **TPEC4-DCM** crystal can be used as evidence for this point. Different from the CH/π interaction in **TPEC4-THF**, only intermolecular/intramolecular hydrogen bonding interactions existed in **TPEC4-DCM** (Fig. S6 and S7, ESI†). Compared with the face to face arrangement of TPE moiety in **TPEC4-THF**, the different one by one form was observed in the structure of **TPEC4-DCM**. To the compound **TPEC4**, the alkoxyl linkage was connected on the two neighboring *ortho* carbons of the two phenyl moieties at the same ethylene carbon which could form a steric hindrance on one side of the TPE plane. When the **TPEC4** molecules packing, the one side bulky group can separate the two adjacent TPE cores, as the result, the **TPEC4** molecules will arrange one by one or face to face which consist with the two crystal structures of **TPEC4** (Fig. 4). The distance of the two C=C bonds of **TPEC4** molecules are *ca.* 0.54 nm (**TPEC4-THF**) and *ca.* 0.90 nm (**TPEC4-DCM**) separately. Generally, the luminescent property is closely related to the package of TPE moiety. However, no obviously different fluorescence spectra of **TPEC4-DCM** (λ_{em} = 405 nm) and **TPEC4-THF** (λ_{em} = 400 nm) in crystal state were observed (Fig. 4). The blue-shifted emissions of two kind of crystals mainly attribute to the similar geometrical rigid crystal

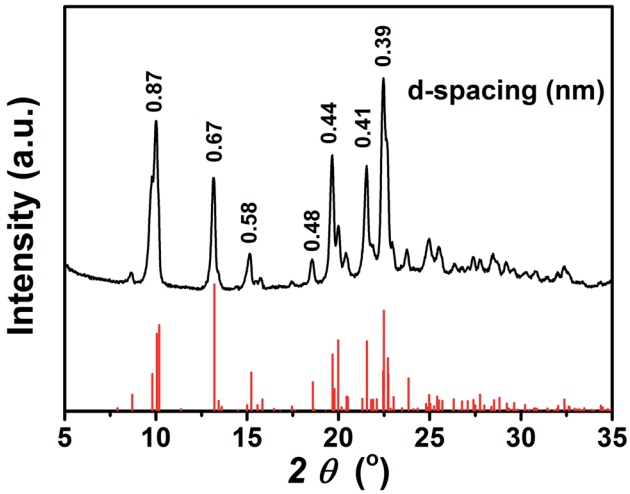

Fig. 5 XRD pattern of **TPEC4** particles formed from DMSO/H_2O mixture (f_w = 60%) (black), together with the simulated powder diffraction pattern on the basis of X-ray crystallographic data (red).

environment which could be proved by the following evidences. (1) Comparing the dihedral angles between the four phenyl rings and the C=C bond, the conformations of the **TPEC4** in **TPEC4-DCM** and **TPEC4-THF** are similar which consists their emission properties. The packing models of the **TPEC4** molecules adopted have limited effects on their emission. (2) The absorption spectra did not change obviously when the emission shifted to shorter wavelength. In the UV-Vis spectrum, electrons are absorbing energy means that the electrons are going to excited state from its ground state, which indicates that the **TPEC4** is having energy band gap. Therefore, the energy band gap can be determine by absorption wavelength. As shown in the UV-Vis spectrum (Fig. S1, ESI†), the spectra are almost the same, except the abnormal absorption spectra (f_w = 55, 60%) which may attribute to the particles formed in these situations make the scattering greater than the absorption. Thus, the fact of the similarity in the absorption indicates that the energy gap of the **TPEC4** was not affected by the assembly.

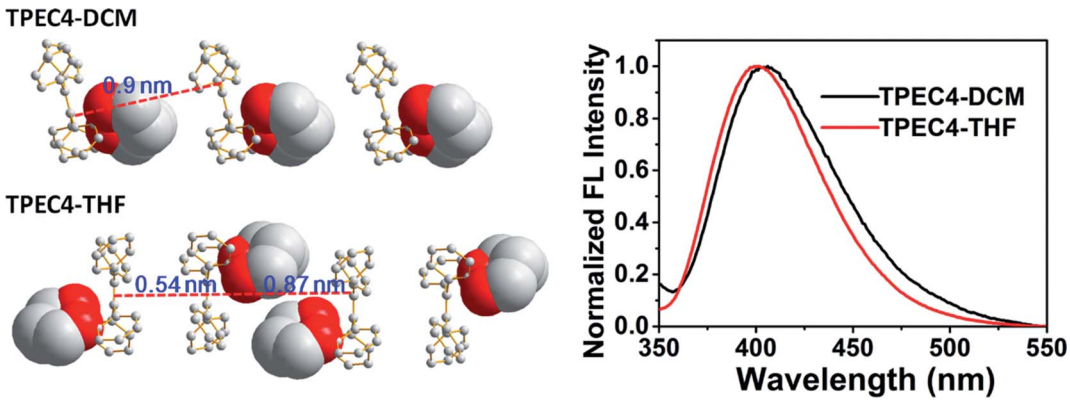

Fig. 4 The packing modes of **TPEC4** in **TPEC4-DCM** and **TPEC4-THF** with non-related hydrogens omitted for clarity and normalized fluorescence spectra of **TPEC4-DCM** and **TPEC4-THF** in crystal state. λ_{ex}: 330 nm (5 nm, 5 nm); 293 K.

Luminescent properties and aggregation behaviour of the TPEC4 in DMSO/H_2O mixture

To further investigate the aggregation behaviour of the **TPEC4** with blue-shifted emission, the particles formed in DMSO/H_2O mixture with $f_w = 60\%$ (concentration: 50 μM) were obtained by centrifugation. Fig. 5 shows that the XRD patterns of the as prepared freeze-dried sample is identical with the simulated powder diffraction pattern on the basis of X-ray crystallographic data of the **TPEC4-THF** crystals, which indicated that the molecular packing of **TPEC4** with blue-shifted emission is an ordered face to face structure. To determine the structure of the aggregated particles with red-shifted emission under higher water fraction, the XRD pattern of the particles formed in DMSO/H_2O mixture with higher f_w (90%) was obtained. Several sharp peaks appeared in the XRD pattern, implying that the aggregates (f_w = 90%) had a certain degree of crystallinity (Fig. S8, ESI†). It was also found that the peaks of XRD patterns were assigned to both the simulated XRD pattern of **TPEC4-DCM** and **TPEC4-THF** crystal. As mentioned above, the CH/π interaction and intermolecular/intramolecular hydrogen bonding interactions existed in **TPEC4-THF** and **TPEC4-DCM** crystal respectively. Thus, the mixed XRD pattern indicates that

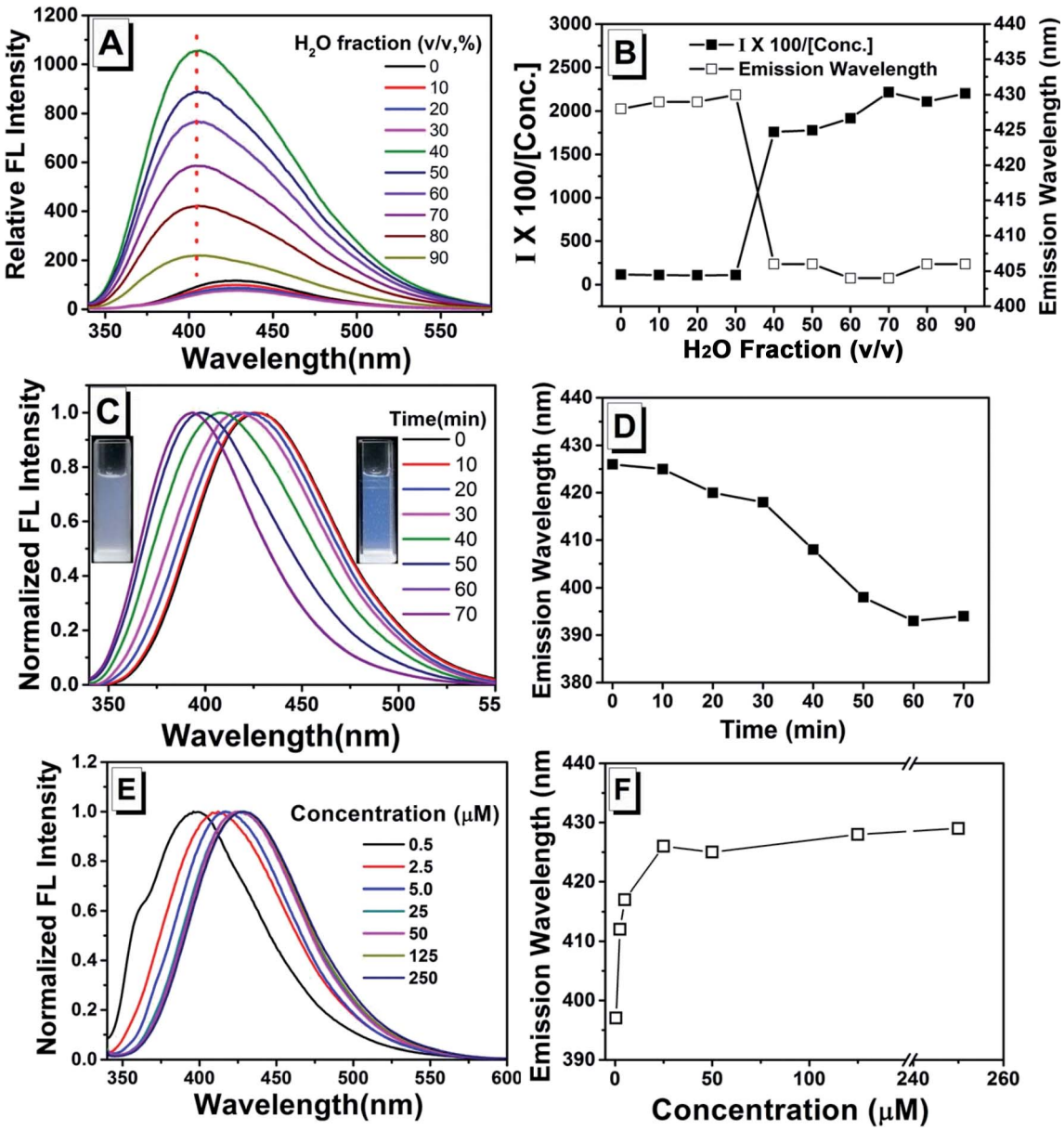

Fig. 6 (A) Fluorescence spectra and (B) plots of the emission peak and fluorescence intensity at maximum emission of **TPEC4** in DMSO/H_2O mixtures with different water fractions in which the water was added continuously (concentration: from 100 to 10 μM); (C) the normalized spontaneous change of fluorescence spectra of **TPEC4** in DMSO/H_2O mixture (f_w = 90%) (concentration: 50 μM) and (D) the plots of the emission wavelength against time; (E) the fluorescence spectra of **TPEC4** in DMSO/H_2O mixture ($f_w = 90\%$) in different concentration (from 0.5 to 250 μM) and (F) the plots of the emission wavelength against concentration. λ_{ex}: 330 nm (5 nm, 5 nm); 293 K.

the self-assembly in the solution (f_w = 90%) was induced by multiple interactions, in which the CH/π and intermolecular/intramolecular hydrogen bonding interactions. As a result, various aggregation packing modes induced the mixed broad emission spectrum. In addition, the disordered aggregation also occurred in this condition (f_w = 90%), leading to that the excited and ground states was not strictly limited by the crystal environment anymore. Therefore, the Stokes shift increased and the red shift in the emission band is observed.

To clarify the role of assembly process, the fluorescence spectra of **TPEC4** with the H_2O was consecutively added into the stock solution in DMSO (100 μM) were recorded (the volume of H_2O added each time and the f_w were listed in Table S3†). The emission intensity does not show obvious changes when the f_w increases from 0 to 30% (Fig. 6A and B). With the f_w increased to 40%, **TPEC4** exhibits a blue-shifted emission from *ca.* 425 to 405 nm. But the blue-shifted emission peaks are broad which indicate that the emissions are multiple components. The absorption of the **TPEC4** does not change with $\lambda_{max} \approx 286$ nm when the f_w increases from 0 to 40% which consists with the result mentioned above. But the emission peak does not exhibit red-shift with the f_w increasing further which could contribute to the amorphous aggregation process was depressed with the H_2O consecutively added. Consisting with this conclusion, the emission of **TPEC4** in H_2O–DMSO mixture (f_w = 90%) was found to be time dependent. As shown in Fig. 6C and D, the emission shows a spontaneous blue-shift change from 425 to 393 nm and the solution change from suspension to emulsion. This is a typical derived assembly process that the **TPEC4** molecules in amorphous state were solvated and assembled in a face to face packing driven by the CH/π interactions together with the solvophobic effects. Correspondingly, the fluorescence spectra of fresh prepared **TPEC4** in DMSO–H_2O mixtures with f_w = 90% are concentration dependent. As shown in Fig. 6E and F, with the concentration increasing from 0.5 to 250 μM, the emission peak shifted from 397 to 429 nm. The amorphous aggregation at low concentration will be depressed and predominated at high concentration.

Conclusions

In summary, for AIE luminogens, the aggregation packing mode and the driving force have important effects on their emission. Here, in **TPEC4**, the quadruple CH/π interaction could drive the TPE molecules adopting a face-to-face crystalline packing. The short wavelength emission mainly attributes to the similar geometrical structure at excited and ground states which was limited by the rigid crystal environment. The blue-shifted phenomena in spectra is attribute to this kind of aggregation predominate during the aggregation process. It is difficult to obtain a uniform aggregation structure using the method that the solvent changing from good to poor. The mixed emission derived from various aggregation packing modes is the main reason for the inconsistent fluorescence emission peaks in this article.

Conflicts of interest

There are no conflicts to declare.

Acknowledgements

This research was supported by the Shandong Province Natural Science Foundation (No. ZR2019MB055), the Natural Science Foundation of China (No. 21601107) is gratefully acknowledged.

Notes and references

1 A. Qin and B. Z. Tang, *Aggregation-Induced Emission: Fundamentals*, John Wiley and Sons, New York, 2013.
2 J. Mei, N. L. C. Leung, R. T. K. Kwok, J. W. Y. Lam and B. Z. Tang, *Chem. Rev.*, 2015, **115**, 11718.
3 J. Mei, Y. Hong, J. W. Y. Lam, A. Qin, Y. Tang and B. Z. Tang, *Adv. Mater.*, 2014, **26**, 5429.
4 Y. Hong, J. W. Y. Lam and B. Z. Tang, *Chem. Soc. Rev.*, 2011, **40**, 5361.
5 Y. Hong, J. W. Y. Lam and B. Z. Tang, *Chem. Commun.*, 2009, 4332.
6 D. Ding, K. Li, B. Liu and B. Z. Tang, *Acc. Chem. Res.*, 2013, **46**, 2441.
7 N. L. C. Leung, N. Xie, W. Yuan, Y. Liu, Q. Wu, Q. Peng, Q. Miao, J. W. Y. Lam and B. Z. Tang, *Chem.–Eur. J.*, 2014, **20**, 15349.
8 K. Kokado and K. Sada, *Angew. Chem., Int. Ed.*, 2019, **58**, 8632–8639.
9 A. Qin and B. Z. Tang, *Aggregation-Induced Emission: Applications*, John Wiley and Sons, New York, 2013.
10 Q. Li and Z. Li, *Adv. Sci.*, 2017, **4**, 1600484.
11 J. Yang, L. Li, Y. Yu, Z. Ren, Q. Peng, S. Ye, Q. Li and Z. Li, *Mater. Chem. Front.*, 2017, **1**, 91.
12 J. Li, J. Wang, H. Li, N. Song, D. Wang and B. Z. Tang, *Chem. Soc. Rev.*, 2020, **49**, 1144.
13 B. Li, T. He, X. Shen, D. Tang and S. Yin, *Polym. Chem.*, 2019, **10**, 796.
14 M. Nishio, M. Hirota and Y. Umezawa, *The CH/π interaction. Evidence, Nature, and Consequences*, Wiley-VCH, New York, 1998.
15 M. Nishio, Y. Umezawa, J. Fantini, M. S. Weissd and P. Chakrabartie, *Phys. Chem. Chem. Phys.*, 2014, **16**, 12648.
16 M. Brandl, M. S. Weiss, A. Jabs, J. Suhnel and R. Hilgenfeld, *J. Mol. Biol.*, 2001, **307**, 357.
17 T. Nishikawa, H. Narita, S. Ogi, Y. Satob and S. Yamaguchi, *Chem. Commun.*, 2019, **55**, 14950.
18 M. Nishio, Y. Umezawa, J. Fantini, M. S. Weiss and P. Chakrabarti, *Phys. Chem. Chem. Phys.*, 2014, **16**, 12648.
19 J. E. Anthony, *Chem. Rev.*, 2006, **106**, 5028.
20 D. Lou, X. Lu, M. Zhang, M. Bai and J. Jiang, *Chem. Commun.*, 2018, **54**, 6987.
21 C. Wang and Z. Li, *Mater. Chem. Front.*, 2017, **1**, 2174.